JACS
JOURNAL OF THE AMERICAN CHEMICAL SOCIETY

Article

pubs.acs.org/JACS

Dearomatization-Induced Transannular Cyclization: Synthesis of Electron-Accepting Thiophene-*S*,*S*-Dioxide-Fused Biphenylene

Aiko Fukazawa,*[,†] Hiroya Oshima,[†] Soji Shimizu,[§,∥] Nagao Kobayashi,[§] and Shigehiro Yamaguchi*[,†,‡]

[†]Department of Chemistry, Graduate School of Science and [‡]Institute of Transformative Bio-Molecules (WPI-ITbM), Nagoya University, Furo, Chikusa, Nagoya 464-8602, Japan

[§]Department of Chemistry, Graduate School of Science, Tohoku University, Aoba, Sendai 980-8578, Japan

Supporting Information

ABSTRACT: The transannular cyclization of dehydroannulenes bearing several alkyne moieties in close proximity is a powerful synthetic method for producing polycyclic aromatic hydrocarbons. We report that the reactivity can be switched by the aromaticity of the ring skeletons fused with the dehydroannulene core. Thus, while thiophene-fused bisdehydro[12]annulene **1** was handled as a stable compound in the air at room temperature, the oxidation with *m*-chloroperbenzoic acid from the aromatic thiophene rings to the nonaromatic thiophene-*S*,*S*-dioxides induced the transannular cyclization, even at room temperature, which was completed within 1 day to produce the formal [2 + 2] cycloadduct **3**. This is in stark contrast to the fact that the thermal cyclization of **1** itself required heating at 80 °C for 9 days for completion. Experimental and theoretical studies indicate that the oxidation of even one thiophene ring in **1** sufficiently decreases the activation barrier for the transannular cyclization that proceeds through the 8π and 4π electrocyclic reaction sequence. The thiophene-*S*,*S*-dioxide-fused biphenylene **3** thus produced exhibits a set of intriguing properties, such as a higher electron affinity ($E_{1/2}$ = −1.17 V vs Fc and Fc$^+$) and a stronger fluorescence (Φ_F = 0.20) than the other relevant biphenylene derivatives, which have electron-donating and nonfluorescent characteristics.

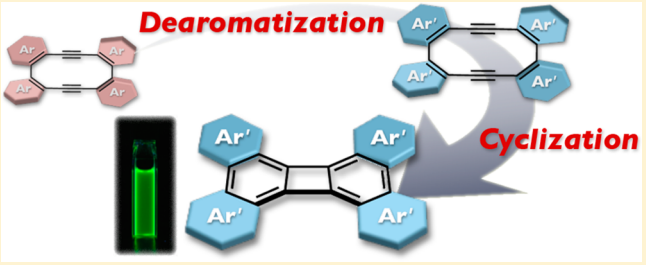

INTRODUCTION

Polycyclic aromatic hydrocarbons (PAHs) play a prominent role in the field of organic electronics as light-emitting materials and semiconductors.[1] A key issue with producing excellent optoelectronic materials based on PAH skeletons is the molecular design that realizes the desirable electronic structure and solid-state packing. These features highly rely on the basic core skeletons in terms of the numbers of fused rings, the modes of ring condensation, and the substituents on the periphery. The incorporation of ring skeletons smaller or larger than benzene or heteroatoms other than carbon also has a significant impact on the electronic structure and the packing mode of PAHs.[2]

Another important issue in this chemistry is how we can construct a highly ring-fused structure. One of the powerful synthetic methods of PAHs is the transannular cyclization of dehydroannulenes, which are π-conjugated macrocycles with alkyne moieties.[3−8] However, this chemistry always encounters a dilemma. While the close proximity of several alkyne moieties fixed in the macrocyclic structure facilitates the reaction, it often results in difficulty in the preparation of the dehydroannulenes themselves because of the low thermal stability.[9] The introduction of aromatic rings to the reactive dehydroannulene skeletons in a fused fashion is a potent approach for their thermodynamic stabilization;[10] however, this ring-fusing strategy sacrifices their inherent reactivity.

As a solution for this dilemma, we envisaged that the selection of a fused ring with the appropriate aromaticity would allow us to tune the balance between the thermodynamic stability of the dehydroannulenes and their reactivity toward the transannular cyclization. In fact, we have found that the thiophene-fused bisdehydro[12]annulene **1** undergoes a transannular cyclization by mild heating even at 80 °C to give a formal [2 + 2] cycloadduct **2** (Figure 1a), while **1** can be readily handled in the air at ambient temperature without special precautions.[11]

This thermal cyclization proceeds through two-step electrocyclic reactions, namely the first 8π electrocyclic reaction to produce a cyclic bis(allene) intermediate, followed by the second 4π electrocyclic reaction. This mechanism is completely different from the photochemical cyclization of **1**, which proceeds through a concerted [2 + 2] cycloaddition.[11] The activation energy of the thermal cyclization of the arene-fused bisdehydro[12]annulenes is highly relevant to the aromaticity of the fused ring on the skeleton, because the first 8π electrocyclic reaction is an inherently energetically unfavorable process that decreases the aromaticity of the fused rings. In compound **1**, the use of the less-aromatic thiophene rings plays

Received: April 8, 2014
Published: May 28, 2014

dx.doi.org/10.1021/ja503499n | J. Am. Chem. Soc. 2014, 136, 8738−8745

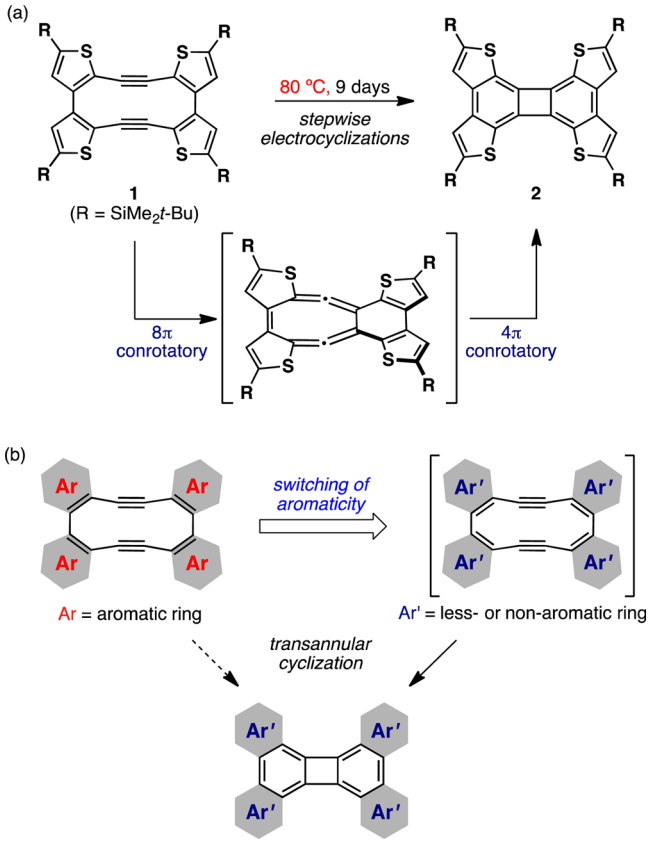

Figure 1. (a) Thermal transannular cyclization of thiophene-fused bisdehydro[12]annulene and (b) control of the reactivity of bisdehydro[12]annulenes by switching the aromaticity of the fused rings.

a crucial role in imparting the balanced stability and reactivity to the dehydroannulene skeleton.

To achieve the explicit control of the reactivity of the dehydroannulenes, we then conceived the switching of the aromaticity of the thiophene rings. We envisioned that the oxidation from the aromatic thiophene to the nonaromatic thiophene-*S*,*S*-dioxide would significantly reduce the activation energy for the transannular cyclization (Figure 1b).[12] Indeed, this strategy enabled us to construct a new highly electron-accepting biphenylene **3** under much milder conditions. We now report the details of the dearomatization-induced transannular cyclization together with a set of intriguing electrochemical and photophysical properties of the thiophene-*S*,*S*-dioxide-fused biphenylenes **3**.

RESULTS AND DISCUSSION

Dearomatization-Induced Transannular Cyclization of Thiophene-Fused Bisdehydro[12]annulene. We first

Scheme 1. Dearomatization-Induced Transannular Cyclization of Bisdehydro[12]annulene 1

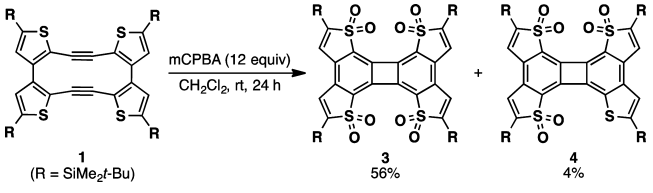

Scheme 2. Reaction of 1 with a Reduced Amount of mCPBA

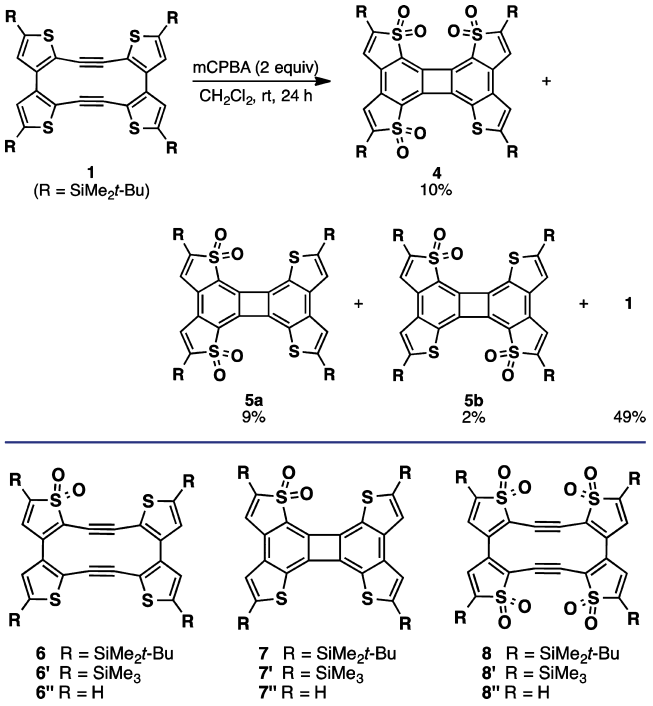

Figure 2. Relevant model compounds of the possible reaction intermediates.

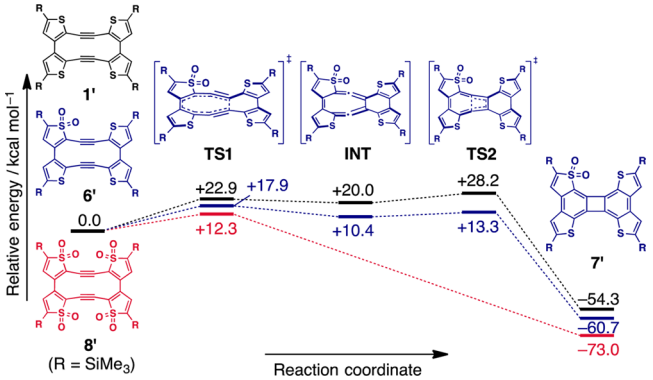

Figure 3. Energy profiles for the transannular cyclization of **1**′ (black) and the partially oxidized and fully oxidized analogues **6**′ (blue) and **8**′ (red) in the ground state calculated at the B3LYP/6-31G(d) level. All energy values are given relative to the initial bisdehydro[12]annulene derivatives.

conducted the oxidation of the fused thiophene rings into the thiophene-*S*,*S*-dioxides in tetrathienobisdehydro[12]annulene **1** using an excess amount of *m*-chloroperbenzoic acid (mCPBA) as the oxidant (Scheme 1).[13−15] The terminal bulky SiMe$_2$*t*-Bu groups in **1** are expected not only to guarantee the solubility of the products but also to electronically facilitate the oxidation of the thiophene rings because of their electron-donating character. We found that the transannular cyclization proceeded even at room temperature. The reaction was completed within 24 h to afford the thiophene-*S*,*S*-dioxide-fused biphenylene **3** and the partially oxidized analogue **4** in 56% and 4% isolated yield, respectively. This result is in stark contrast to the fact that the thermal cyclization of **1** required 9 days at 80 °C for completion.

dx.doi.org/10.1021/ja503499n | J. Am. Chem. Soc. 2014, 136, 8738−8745

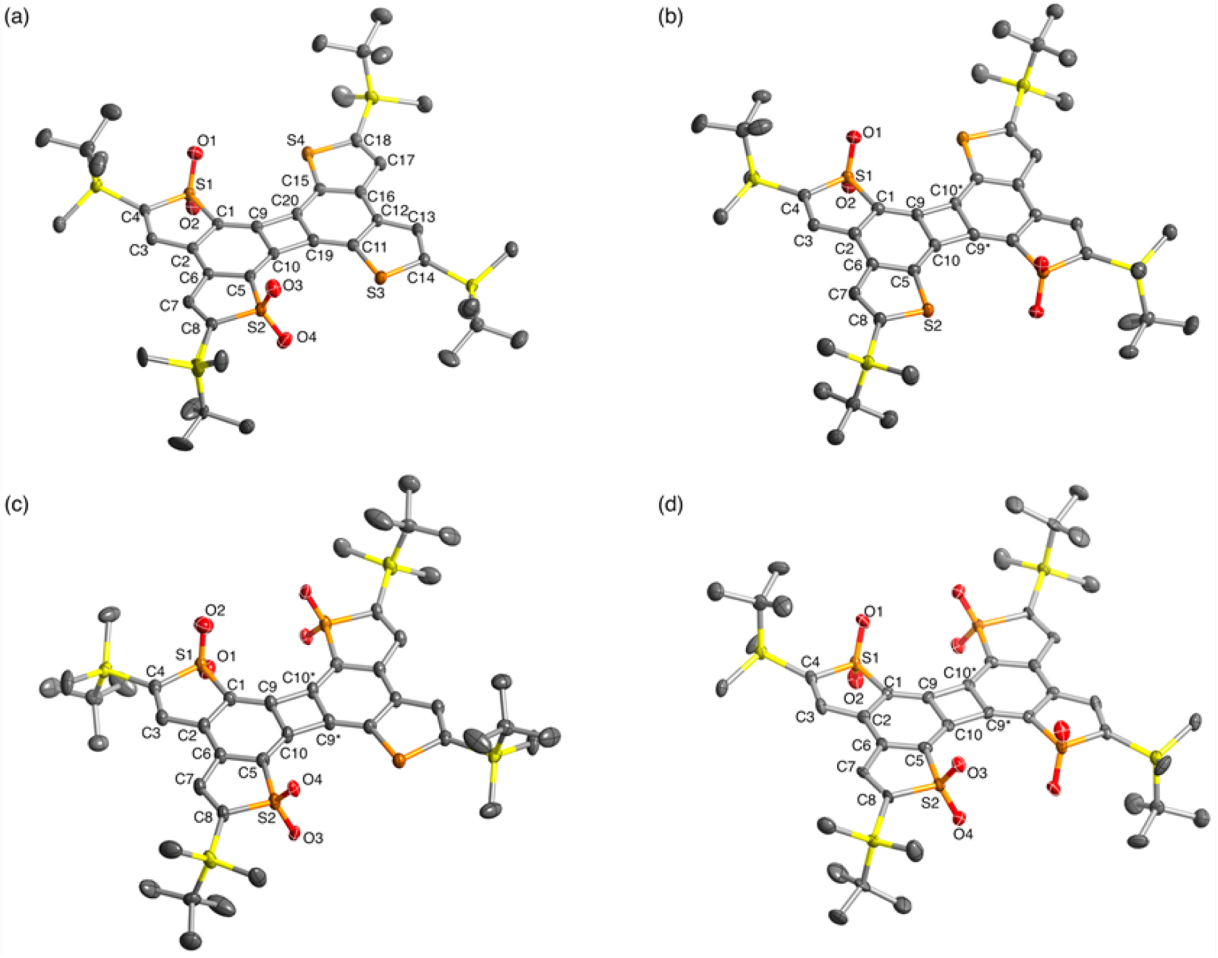

Figure 4. Crystal structures of (a) **5a**, (b) **5b**, (c) **4**, and (d) **3** (50% probability for thermal ellipsoids) with atom labels. Hydrogen atoms are omitted for clarity. The positions of six oxygen atoms in **4** are disordered over the four thiophene rings. Six of the eight oxygen atoms are shown for clarity (see the Supporting Information for details).

Table 1. Selected Bond Lengths (Å) of a Series of Biphenylene Derivatives

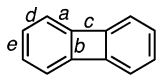

compound	*a*	*b*	*c*	*d*	*e*
2[a]	C1−C9 1.383(4)	C9−C10 1.415(4)	C9−C10* 1.516(4)	C1−C2 1.420(4)	C2−C6 1.407(4)
	C5−C10 1.378(4)			C5−C6 1.434(4)	
5a	C1−C9 1.353(3)	C9−C10 1.447(3)	C9−C20 1.488(3)	C1−C2 1.439(3)	C2−C6 1.376(3)
	C5−C10 1.358(3)	C19−C20 1.409(3)	C10−C19 1.492(3)	C5−C6 1.443(3)	C12−C16 1.422(3)
				C11−C12 1.422(3)	
				C15−C16 1.417(3)	
5b	C1−C9 1.366(5)	C9−C10 1.422(5)	C9−C10* 1.497(5)	C1−C2 1.422(5)	C2−C6 1.411(5)
	C5−C10 1.375(5)			C5−C6 1.446(5)	
4	C1−C9 1.365(3)	C9−C10 1.429(3)	C9−C10* 1.497(3)	C1−C2 1.432(3)	C2−C6 1.390(3)
	C5−C10 1.359(3)			C5−C6 1.421(3)	
3	C1−C9 1.347(8)	C9−C10 1.459(8)	C9−C10* 1.496(8)	C1−C2 1.422(8)	C2−C6 1.389(8)
	C5−C10 1.359(8)			C5−C6 1.426(8)	
biphenylene[b]	1.372(2)	1.426(3)	1.514(3)	1.423(3)	1.385(4)

[a]See ref 11. [b]See ref 17.

Mechanistic Insights. To elucidate the impact of the oxidation of the thiophene rings on the reactivity toward the transannular cyclization, we next conducted a reaction with a reduced amount of mCPBA (2 equiv) (Scheme 2). After being stirred for 24 h at room temperature, the reaction was stopped and the mixture was subjected to column chromatography to give partially oxidized tetrathienobiphenylenes **5a**, **5b**, and **4**, which contain two or three thiophene-*S*,*S*-dioxide rings, in 9%, 2%, and 10% yields, respectively. While the unreacted starting material **1** was also recovered in 49%, we could not obtain any

dx.doi.org/10.1021/ja503499n | J. Am. Chem. Soc. 2014, 136, 8738−8745

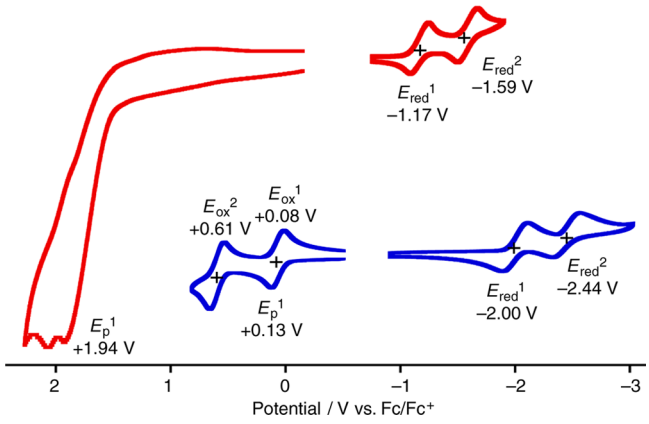

Figure 5. Cyclic voltammograms of **3** (red) and **2** (blue) measured in CH_2Cl_2 for oxidation and in THF for reduction (sample, 1 mM; $Bu_4N^+PF_6^-$, 0.1 M; scan rate, 100 mV s^{-1}). Fc = ferrocene.

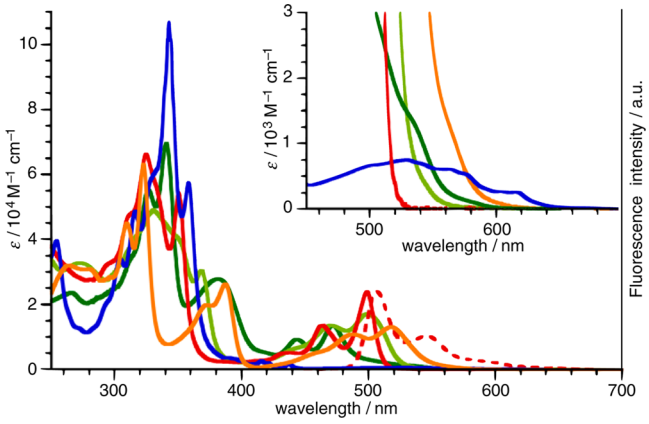

Figure 6. UV−vis absorption (solid line) and fluorescence spectra (dashed line) of **3** (red), **5a** (green), **5b** (yellow), **4** (light green), and **2** (blue) in THF.

monothiophene-oxidized product. The isolation of the biphenylenes **4** and **5** implies that the transannular cyclization is promoted at room temperature by the oxidation of not all of the thiophene rings but of a part of the four thiophene rings.

To gain deeper insights into the effect of the oxidation on the reactivity, density functional theory (DFT) calculations of some possible intermediates **6**−**8** (Figure 2) were conducted at the B3LYP/6-31G(d) level using their respective model compounds **6′**−**8′** that have $SiMe_3$ groups in place of the *t*-$BuMe_2Si$ groups. Notably, the highest occupied molecular orbital (HOMO) energy level of the monothiophene-oxidized tetrathienobiphenylene **7′** (−4.90 eV) lies much higher than those of the monothiophene-oxidized or nonoxidized bisdehydro[12]annulenes **6′** (−5.58 eV) and **1′** (−5.37 eV). This comparison suggests that **7** can be more easily oxidized than can **6** and **1**. Thus, in light of the fact that **4** and **5** were isolated with the recovery of **1**, it is likely that the cyclization is triggered at room temperature by the oxidation of only one thiophene ring in **1**, and the resulting **7** is further oxidized to **5** or **4**.

To elucidate the reaction mechanism, the reactions of the partially or fully oxidized thiophene-fused bisdehydro[12]-annulenes **6′** and **8′** were theoretically investigated. The geometry optimization of the possible intermediates and transition states as well as the intrinsic reaction coordinate (IRC) analysis were conducted at the B3LYP/6-31G(d) level of theory. The results are shown in Figure 3 together with that of **1′**, a model compound for **1**,[11] for comparison. The transannular cyclizations of **6′** and **8′** proceed in a similar manner to that of **1′**, namely the 8π and 4π electrocyclic reaction sequence, although we could not find any intermediate in the reaction course of the fully oxidized **8′** because of its shallow potential energy surface. Notably, the net activation energies (ΔE) for the two-step cyclizations become lower as the number of the oxidized thiophene rings increases (+22.9 kcal mol^{-1} from **1′** to **2′**; +17.9 kcal mol^{-1} from **6′** to **7′**; +12.3 kcal mol^{-1} from **8′** to **3′**).[16] This trend clearly demonstrates that the dearomatization of the fused ring skeleton significantly reduces the activation barrier of the transannular cyclization.[11] It should be noted that the dearomatization of even one thiophene ring has an impact that is sufficient enough to trigger cyclization at room temperature.

X-ray Crystallographic Analysis. The structures of **3**, **4**, **5a**, and **5b** were verified by X-ray crystallographic analyses (Figure 4 and Table 1). In the partially oxidized **4**, six oxygen atoms were disordered over the eight possible positions on four thiophene rings and therefore were refined using the appropriate disordered model (see the Supporting Information for details). The seven ring-fused skeletons in all of these compounds have a highly coplanar geometry with the dihedral angles between the adjacent thiophene rings of 5.79°, 3.42−9.26°, 6.02°, and 3.60° for **3**, **5a**, **5b**, and **4**, respectively, indicative of the effective extension of the π conjugation. In addition, the fully oxidized compound **3** has a greater contribution to the [4]radialene-like resonance form in the central biphenylene skeleton than those in the nonoxidized analogue **2**[11] and a parent biphenylene,[17] despite the expense of losing the aromaticity of the benzene rings (Table 1). Thus, the lengths of the exocyclic C−C bonds *a* in **3** were 1.347(8) Å and 1.359(8) Å, which are shorter than those of **2** and the parent biphenylene (**2**, 1.383(4) Å and 1.378(4) Å; biphenylene, 1.372(2) Å). The bond-length alternation of the central four-membered rings in **3** also becomes smaller than those in **2** and the parent biphenylene. While the bond lengths of the C−C bond *b* in **3**, **2**, and biphenylene are 1.459(8) Å, 1.415(4) Å, and 1.426(3) Å, respectively, the C−C bond *c* in **3**, **2**, and biphenylene are 1.496(8) Å, 1.516(4) Å, and 1.514(3) Å, respectively. These differences in the bond lengths indicate that the fused thiophene-*S*,*S*-dioxides significantly perturb the electronic structure of the biphenylene moiety. To evaluate the extent of the perturbation, we calculated the nucleus independent chemical shift (NICS)[18] of **3** using the crystal structure at the HF/6-31+G(d,p) level. The NICS(1) values of the benzene and cyclobutadiene rings in **3** are −6.38 ppm and +5.23 ppm, while those in **2** are −8.13 ppm and +15.7 ppm, respectively.

Properties and Electronic Structures of Tetrathienobiphenylenes. The most notable electronic effect of the dearomatization of the thiophene ring in **3** is its enhanced electron-accepting properties. In the cyclic voltammogram (Figure 5), **3** showed reversible two-step redox waves with the half-wave potentials $E_{1/2}$ of −1.17 and −1.59 V (vs Fc and Fc^+) attributable to the two-electron reduction and an irreversible oxidation wave with the peak potential E_p of +1.94 V (vs Fc and Fc^+). The reduction potentials of **3** are much more positive than those of **2** ($E_{1/2}$ = −2.00 and −2.44 V), suggesting a significantly lower-lying lowest unoccupied molecular orbital (LUMO) due to the strong electron-withdrawing effect of the

dx.doi.org/10.1021/ja503499n | J. Am. Chem. Soc. 2014, 136, 8738−8745

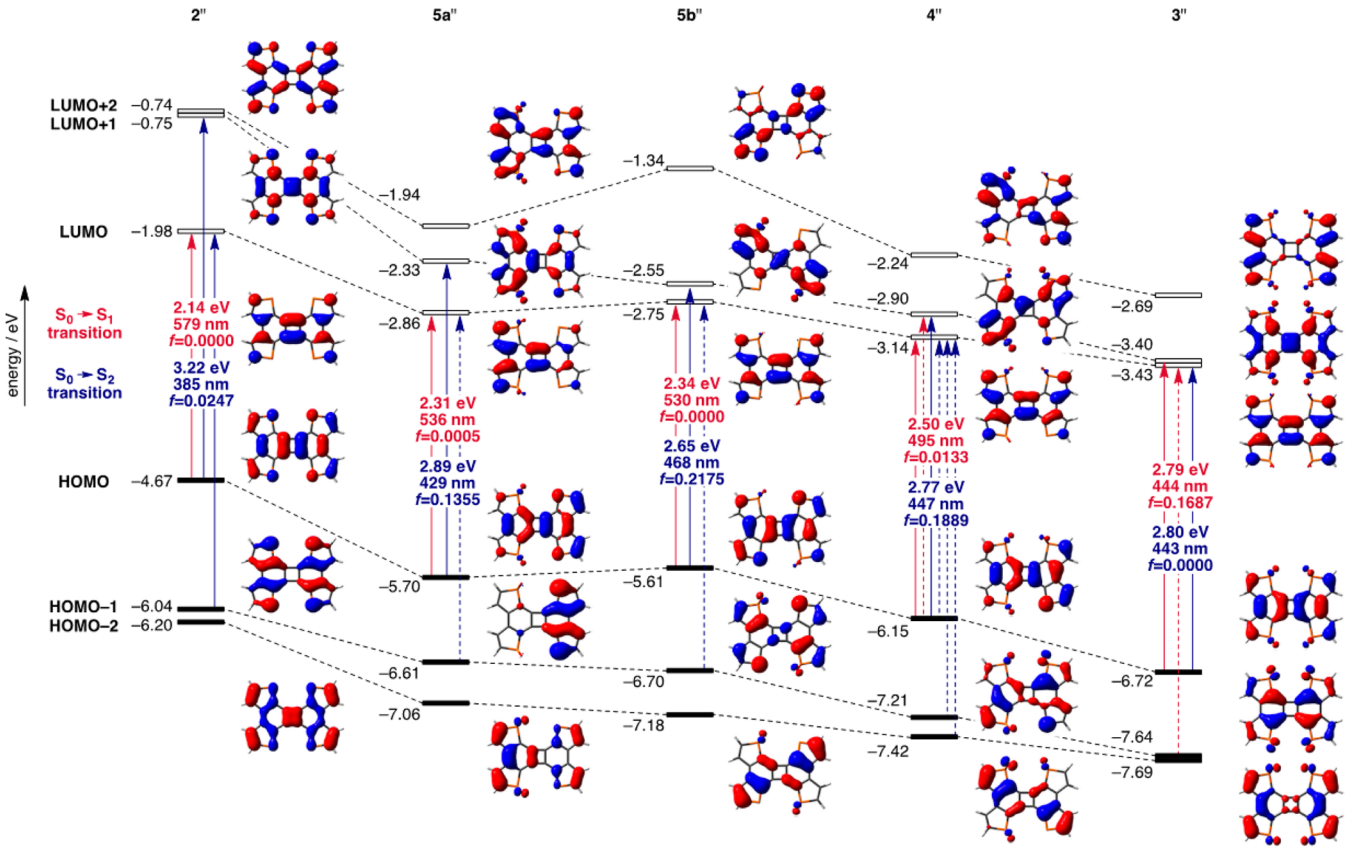

Figure 7. Energy diagrams and the pictorial representations of the selected Kohn−Sham molecular orbitals for the tetrathienobiphenylene derivatives **2″**, **3″**, **4″**, **5a″**, and **5b″** calculated at the B3LYP/6-31G(d) level, and their lowest- and second-lowest-energy transitions estimated by time-dependent (TD)-DFT calculations at the B3LYP/6-31G(d) level. In these model compounds, hydrogen atoms were used in place of *t*-BuMe$_2$Si groups in the corresponding compounds **2**−**5**.

sulfone moieties.[13,19−32] This strong electron-accepting nature is in good contrast to the electron-donating character of **2**.

The oxidized tetrathienobiphenylene **3** also showed intriguing photophysical properties. The UV−vis absorption and fluorescence spectra of the tetrathienobiphenylene derivatives **3**, **4**, **5a**, and **5b** in tetrahydrofuran (THF) are shown in Figure 6 together with the absorption spectrum of **2** for comparison. Tetrathienobiphenylene **2** and its partially oxidized analogues **5a** and **5b** showed very weak longest-wavelength absorption bands similar to the parent biphenylene (biphenylene:[33] λ_{max} = 392 nm, ε = 120 M^{-1} cm^{-1}. **2**: λ_{max} = 616 nm, ε = 260 M^{-1} cm^{-1}. **5a**: λ_{max} = 535 nm (shoulder), ε = 1300 M^{-1} cm^{-1}. **5b**: λ_{max} = 565 nm (shoulder), ε = 1100 M^{-1} cm^{-1}),[34,35] whereas the longest-wavelength absorption band of the fully oxidized **3** was significantly blue-shifted with a much larger molar absorption coefficient (λ_{max} = 499 nm, ε = 2.40 × 10^4 M^{-1} cm^{-1}). Moreover, the fully oxidized **3** exhibited a pronounced green fluorescence (λ_{em} = 507 nm) in THF, in contrast to the fact that the parent biphenylene,[33,34,36] thiophene-fused biphenylene **2**, and the partially oxidized analogues **5b** and **4** did not show visible fluorescence. The fluorescence spectrum of **3** exhibited a good mirror image with the absorption spectrum and its Stokes shift was very small ($\Delta\lambda$ = 8 nm, 316 cm^{-1}) because of the rigid π-conjugated framework. Its fluorescence quantum yield Φ_F was 0.20. The time-resolved fluorescence spectroscopy showed a single exponential decay from the excited singlet state, and the fluorescence lifetime (τ_s) of **3** was 0.26 ns. The radiative decay rate constant calculated from the Φ_F and τ_s was 7.7 × 10^8 s^{-1}, which is a relatively high value among the organic molecules and is indicative of a large oscillator strength for the $S_1 \rightarrow S_0$ transition.

To explain why **3** showed completely different characteristics in the electronic spectra compared to those of **2** and the parent biphenylene, the TD-DFT calculations of their model compounds **2″** and **3″** were performed. The results are shown in Figure 7. The tetrathienobiphenylene **2″** has a symmetry-forbidden first electronic transition ($^1B_{3g}$, 2.14 eV, f = 0.0000) and a symmetry-allowed second transition ($^1B_{1u}$, 3.22 eV, f = 0.0247) similar to that of the parent biphenylene.[34,36] The forbidden nature of the $S_0 \rightarrow S_1$ transition is consistent with the nonfluorescent nature of **2**. In stark contrast, the characteristics of the first and second electronic transitions of the fully oxidized tetrathienobiphenylene **3′** (S_1: $^1B_{2u}$, 2.79 eV, f = 0.1687; S_2: $^1B_{1g}$, 2.80 eV, f = 0.0000) are opposite to those of **2″**. This difference, particularly the larger oscillator strength (f) of the $S_0 \rightarrow S_1$ transition, is consistent with the large molar absorption coefficient ε of **3** for the longest-wavelength absorption (Figure 6) and is responsible for the intense fluorescence. The switching of the excited-state characteristics is reasonably explained by the electron-withdrawing effect of the sulfone moieties, which more significantly affect the LUMO +1 rather than the LUMO. As a consequence, these molecular orbitals (MOs) are degenerated. Importantly, this degeneracy occurs only for the fully oxidized **3′**.

The electronic spectra of the biphenylene derivatives have attracted particular attention as one of the 4*N*-electron cyclic π-conjugated systems.[34−38] To gain further experimental insight into the perturbation of the electronic transitions by oxidation

dx.doi.org/10.1021/ja503499n | J. Am. Chem. Soc. 2014, 136, 8738−8745

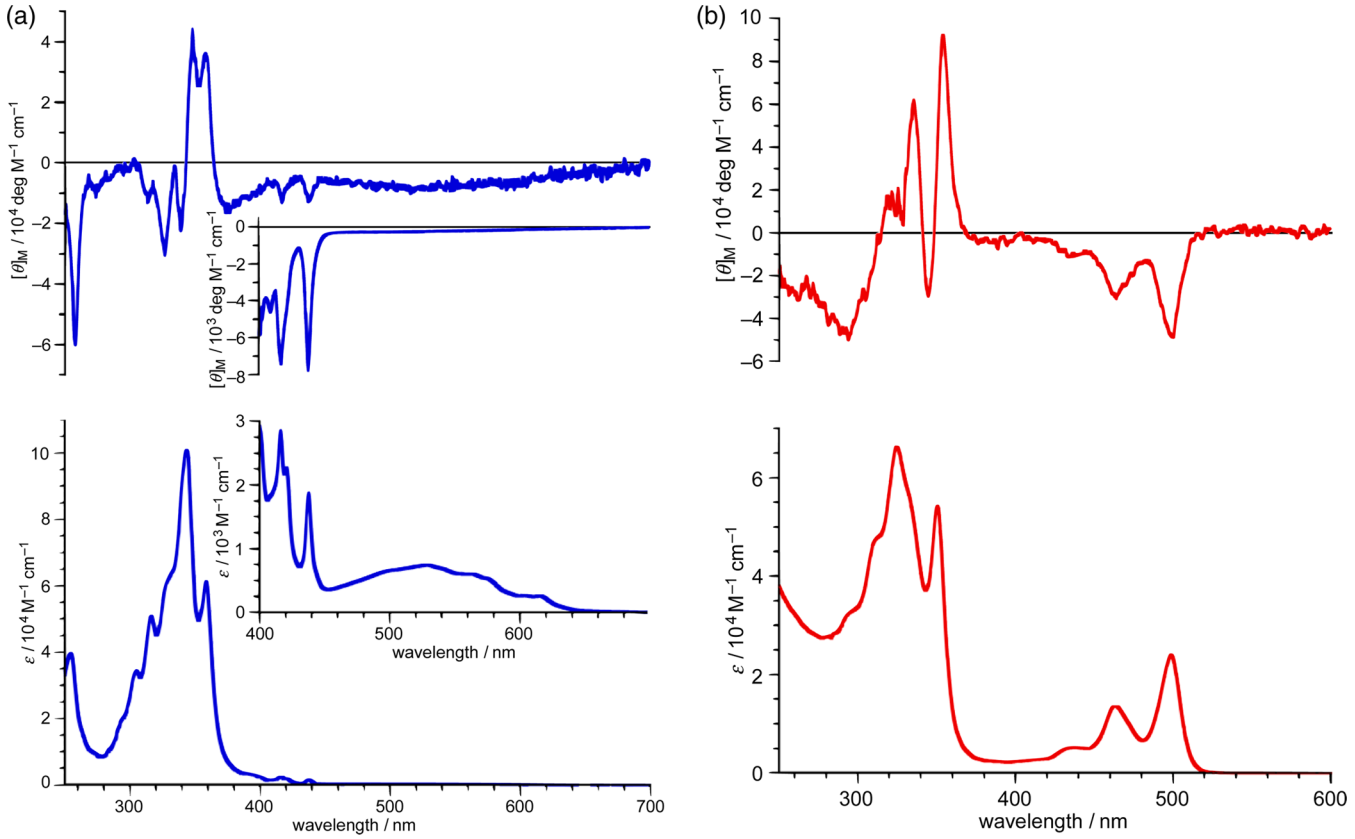

Figure 8. Magnetic circular dichroism (MCD) (top) and UV−vis absorption spectra (bottom) of (a) **2** and (b) **3**. The inset figures show the enlarged MCD and UV−vis absorption spectra.

of the fused thiophene rings, we also evaluated the spectral characteristics with MCD spectroscopy[39] (Figure 8). In light of the molecular symmetry, all of the signals of biphenylene and its derivatives are contributions of Faraday *B* terms, and their MCD spectra can be interpreted on the basis of Michl's 4*N* perimeter model,[37] in which six frontier MOs, HOMO−2, HOMO−1, HOMO, LUMO, LUMO+1, and LUMO+2, play a key role in the electronic transitions. In Michl's terminology, these MOs are referred to as *h*−, *h*+, *s*−, *s*+, *l*−, and *l*+, respectively, which are derived from the symmetry perturbation of the degenerate HOMO, singly-occupied molecular orbital (SOMO), and LUMO of an ideal [12]annulene perimeter. The five excited states, S, N_1, P_1, N_2, and P_2, are then considered. The S band corresponds to a transition from *s*− (HOMO) to *s* + (LUMO), which is of an intrashell nature; therefore, this band is very weak, and generally a negative MCD signal is observed. N_1 and P_1 bands comprise configuration interactions between states arising from the transitions from *s*− (HOMO) to *l*− (LUMO+1) and from *h*+ (HOMO−1) to *s*+ (LUMO), so that cancellation and intensification results in a weak N_1 band and an intense P_1 band. Weak N_2 and intense P_2 bands also can be similarly interpreted based on configuration interactions between states arising from the transitions from *s*− (HOMO) to *l*+ (LUMO+2) and from *h*− (HOMO−2) to *s* + (LUMO). These bands appear, in higher energy, in the order of S, N_1, P_1, N_2, and P_2. The absorption and MCD spectra of **2** can be interpreted as an exemplary case of a 4*N*-electron system. The broad, almost negligible absorption of **2** ranging from 460 to 640 nm with a negative MCD signal, which is referred to as a positive Faraday *B* term, can be assigned as the S band. The second, well-structured absorption around 420 nm with a distinctive positive Faraday *B* term is of an N_1 band origin, and the significantly intense absorption bands with negative and positive Faraday *B* terms, which are composed of the P_1, N_2, and P_2 bands, follow. These band assignments are supported by the TD-DFT calculations. The MCD spectrum of the oxidized derivative **3** is different from that of **2**. Compound **3** showed strong negative MCD signals corresponding to the band at the longest wavelength. As seen in Figure 7, symmetries of the six frontier orbitals of **2** and **3** are essentially identical, except for the significant stabilization of the LUMO+1 in **3**. On the basis of Michl's interpretation, stabilization of the LUMO+1 (*l*−) reduces configuration interactions for the N_1 and P_1 bands, resulting in a red-shift and intensification of the N_1 band. The intense absorption with an intense positive Faraday *B* term that was observed for **3** around 500 nm can be, therefore, assigned as N_1 band, which overlaps a weak S band. This discussion is also strongly supported by the TD-DFT calculations. These results demonstrate that the fully oxidized **3** retains the electronic characteristics of a biphenylene, which can be explained by Michl's 4*N* perimeter model, although the characteristics of the lowest-energy and second lowest-energy excited states were opposite from those in **2** and in a parent biphenylene.

■ CONCLUSION

We have demonstrated that the transannular cyclization of the tetrathienobisdehydro[12]annulene can be triggered by the oxidation of the fused thiophene rings. This result provides a fundamental concept to tune the reactivity of the dehydroannulenes by switching the aromaticity of the fused rings without sacrificing the stability of the dehydroannulene precursors. The

dx.doi.org/10.1021/ja503499n | *J. Am. Chem. Soc.* 2014, 136, 8738−8745

dearomatization-induced cyclization of **1** enabled us to produce the thiophene-*S*,*S*-dioxide-fused biphenylene **3**. This skeleton has a potential utility as a two-dimensionally expandable π-conjugated core. The strong electron-withdrawing effect of the fused thiophene-*S*,*S*-dioxide moieties has significant impacts on the electronic structure of the biphenylene skeleton so as to impart the attractive properties, such as the highly electron-accepting character with an electrochemical stability and the intense fluorescence with a large radiative decay rate constant. These results indicate the potential of **3** as a scaffold for various applications, including n-type organic semiconducting materials and light-emitting materials. A further study along these lines is now in progress in our laboratory.

■ ASSOCIATED CONTENT

Supporting Information

Experimental procedures, characterization data for all new compounds, additional spectra, results of theoretical calculations, and crystallographic information (CIF) files of compounds **3** and **5**. This material is available free of charge via the Internet at http://pubs.acs.org.

■ AUTHOR INFORMATION

Corresponding Authors

aiko@chem.nagoya-u.ac.jp
yamaguchi@chem.nagoya-u.ac.jp

Present Address

[‖]S.S., Center for Molecular Systems, Department of Chemistry and Biochemistry, Graduate School of Engineering, Kyushu University, Fukuoka 819-0395, Japan.

Notes

The authors declare no competing financial interest.

■ ACKNOWLEDGMENTS

This work was supported by CREST, JST, and ACT-C, JST. H.O. thanks the Nagoya University Program for Leading Graduate Schools "Integrative Graduate Education and Research Program in Green Natural Science."

■ REFERENCES

(1) (a) Berresheim, A. J.; Müller, M.; Müllen, K. *Chem. Rev.* **1999**, *99*, 1747−1786. (b) Watson, M. D.; Fechtenkötter, A.; Müllen, K. *Chem. Rev.* **2001**, *101*, 1267−1300. (c) Bendikov, M.; Wudl, F.; Perepichka, D. F. *Chem. Rev.* **2004**, *104*, 4891−4946. (d) Anthony, J. E. *Chem. Rev.* **2006**, *106*, 5028−5048. (e) Sergeyev, S.; Pisula, W.; Geerts, Y. H. *Chem. Soc. Rev.* **2007**, *36*, 1902−1929. (f) Murphy, A. R.; Fréchet, J. M. *Chem. Rev.* **2007**, *107*, 1066−1096. (g) Weil, T.; Vosch, T.; Hofkens, J.; Peneva, K.; Müllen, K. *Angew. Chem., Int. Ed.* **2010**, *49*, 9068−9093.

(2) (a) Miljanic, O. S.; Vollhardt, K. P. C. [*N*]Phenylenes: A Novel Class of Cyclohexatrienoid Hydrocarbons. In *Carbon-Rich Compounds*; Haley, M. M., Tykwinski, R. R., Eds.; Wiley-VCH: Weinheim, Germany, 2006; pp 140−197. (b) Wu, Y.-T.; Siegel, J. S. *Chem. Rev.* **2006**, *106*, 4843−4867.

(3) Mitchell, R. H.; Sondheimer, F. *Tetrahedron* **1970**, *26*, 2141−2150.

(4) Staab, H. A.; Ipaktschi, J.; Nissen, A. *Chem. Ber.* **1971**, *104*, 1182−1190.

(5) Bergman, R. G. *Acc. Chem. Res.* **1973**, *6*, 25−31.

(6) Umeda, R.; Hibi, D.; Miki, K.; Tobe, Y. *Pure Appl. Chem.* **2010**, *82*, 871−878.

(7) (a) Sun, Z.; Huang, K.-W.; Wu, J. *Org. Lett.* **2010**, *12*, 4690−4693. (b) Sun, Z.; Huang, K.-W.; Wu, J. *J. Am. Chem. Soc.* **2011**, *133*, 11896−11899.

(8) Chakraborty, M.; Tessier, C. A.; Youngs, W. J. *J. Org. Chem.* **1999**, *64*, 2947−2949.

(9) Wolovsky, R.; Sondheimer, F. *J. Am. Chem. Soc.* **1962**, *84*, 2844−2845.

(10) (a) Kennedy, R. D.; Lloyd, D.; McNab, H. *J. Chem. Soc., Perkin Trans. 1* **2002**, 1601−1621. (b) Spitler, E. L.; Johnson, C. A., II; Haley, M. M. *Chem. Rev.* **2006**, *106*, 5344−5386.

(11) Fukazawa, A.; Oshima, H.; Shiota, Y.; Takahashi, S.; Yoshizawa, K.; Yamaguchi, S. *J. Am. Chem. Soc.* **2013**, *135*, 1731−1734.

(12) For the dearomatization of the thiophene ring by sulfur oxidation, see: Tanaka, K.; Wang, S.; Yamabe, T. *Synth. Met.* **1989**, *30*, 57−65.

(13) (a) Barbarella, G.; Favaretto, L.; Zambianchi, M.; Pudova, O.; Arbizzani, C.; Bongini, A.; Mastragostino, M. *Adv. Mater.* **1998**, *10*, 551−554. (b) Barbarella, G.; Pudova, O.; Arbizzani, C.; Mastragostino, M.; Bongini, A. *J. Org. Chem.* **1998**, *63*, 1742−1745. (c) Barbarella, G.; Favaretto, L.; Sotgiu, G.; Zambianchi, M.; Arbizzani, C.; Bongini, A.; Mastragostino, M. *Chem. Mater.* **1999**, *11*, 2533−2541.

(14) Suh, M. C.; Jiang, B.; Tilley, T. D. *Angew. Chem., Int. Ed.* **2000**, *39*, 2870−2873.

(15) Pappenfus, T. M.; Melby, J. H.; Hansen, B. B.; Sumption, D. M.; Hubers, S. A.; Janzen, D. E.; Ewbank, P. C.; McGee, K. A.; Burand, M. W.; Mann, K. R. *Org. Lett.* **2007**, *9*, 3721−3724.

(16) The DFT calculations for the transannular cyclization of the model compounds **1″**, **6″**, and **8″** having hydrogen atoms in place of *t*-BuMe$_2$Si groups also gave similar results. See the Supporting Information for details.

(17) Fawcett, J. K.; Trotter, J. *Acta Crystallogr.* **1966**, *20*, 87−93.

(18) Nucleus-independent chemical shift (NICS) is an index for aromaticity based on the magnetic shielding computed at chosen points in the vicinity of the rings. Larger absolute values with negative and positive signs indicate higher aromaticity and antiaromaticity, respectively, of the certain ring. For details, see: (a) Schleyer, P. v. R.; Maerker, C.; Dransfeld, A.; Jiao, H.; Van Eikema Hommes, N. J. R. *J. Am. Chem. Soc.* **1996**, *118*, 6317−6318. (b) Corminboeuf, C.; Heine, T.; Seifert, G.; Schleyer, P. v. R.; Weber, J. *Phys. Chem. Chem. Phys.* **2004**, *6*, 273−276. (c) Fallah-Bagher-Shaldael, H.; Wannere, C. S.; Corminboeuf, C.; Puchta, R.; Schleyer, P. v. R. *Org. Lett.* **2006**, *8*, 863−866.

(19) Dell, E. J.; Campos, L. M. *J. Mater. Chem.* **2012**, *22*, 12945−12952 and the references therein.

(20) (a) Barbarella, G.; Favaretto, L.; Sotgiu, G.; Zambianchi, M.; Bongini, A.; Arbizzani, C.; Mastragostino, M.; Anni, M.; Gigli, G.; Cingolani, R. *J. Am. Chem. Soc.* **2000**, *122*, 11971−11978. (b) Barbarella, G.; Favaretto, L.; Sotgiu, G.; Antolini, L.; Gigli, G.; Cingolani, R.; Bongini, A. *Chem. Mater.* **2001**, *13*, 4112−4122. (c) Mazzeo, M.; Vitale, V.; Sala, F. D.; Pisignano, D.; Anni, M.; Barbarella, G.; Favaretto, L.; Zanelli, A.; Cingolani, R.; Gigli, G. *Adv. Mater.* **2003**, *15*, 2060−2063. (d) Barbarella, G.; Favaretto, L.; Zanelli, A.; Gigli, G.; Mazzeo, M.; Anni, M.; Bongini, A. *Adv. Funct. Mater.* **2005**, *15*, 664−670. (e) Mariano, F.; Mazzeo, M.; Duan, Y.; Barbarella, G.; Favaretto, L.; Carallo, S.; Cingolani, R.; Gigli, G. *Appl. Phys. Lett.* **2009**, *94*, 063510.

(21) Beaupré, S.; Leclerc, M. *Adv. Funct. Mater.* **2002**, *12*, 192−196.

(22) (a) Perepichka, I. I.; Perepichka, I. F.; Bryce, M. R.; Pålsson, L.-O. *Chem. Commun.* **2005**, 3397−3399. (b) King, S. M.; Perepichka, I. I.; Perepichka, I. F.; Dias, F. B.; Bryce, M. R.; Monkman, A. P. *Adv. Funct. Mater.* **2009**, *19*, 586−591.

(23) Suzuki, Y.; Okamoto, T.; Wakamiya, A.; Yamaguchi, S. *Org. Lett.* **2008**, *10*, 3393−3396.

(24) (a) Huang, T.-H.; Lin, J. T.; Chen, L.-Y.; Lin, Y.-T.; Wu, C.-C. *Adv. Mater.* **2006**, *18*, 602−606. (b) Huang, T.-H.; Whang, W.-T.; Shen, J. Y.; Wen, Y.-S.; Lin, J. T.; Ke, T.-H.; Chen, L.-Y.; Wu, C.-C. *Adv. Funct. Mater.* **2006**, *16*, 1449−1456.

(25) Miguel, L. S.; Matzger, A. J. *J. Org. Chem.* **2008**, *73*, 7882−7888.

(26) Moss, K. C.; Bourdakos, K. N.; Bhalla, V.; Kamtekar, K. T.; Bryce, M. R.; Fox, M. A.; Vaughan, H. L.; Dias, F. B.; Monkman, A. P. *J. Org. Chem.* **2010**, *75*, 6771−6781.

(27) Afonina, I.; Skabara, P. J.; Vilela, F.; Kanibolotsky, A. L.; Forgie, J. C.; Bansal, A. K.; Turnbull, G. A.; Samuel, I. D. W.; Labram, J. G.; Anthopoulos, T. D.; Coles, S. J.; Hursthouse, M. B. *J. Mater. Chem.* **2010**, *20*, 1112−1116.
(28) Amir, E.; Sivanandan, K.; Cochran, J. E.; Cowart, J. J.; Ku, S.-Y.; Seo, J. H.; Chabinyc, M. L.; Hawker, C. J. *J. Polym. Sci., Part A: Polym. Chem.* **2011**, *49*, 1933−1941.
(29) Ren, Y.; Baumgartner, T. *J. Am. Chem. Soc.* **2011**, *133*, 1328−1340.
(30) Duan, Z.; Huang, X.; Fujii, S.; Kitaura, H.; Nishioka, Y. *Chem. Lett.* **2012**, *41*, 363−365.
(31) Tsai, C.-H.; Chirdon, D. N.; Maurer, A. B.; Bernhard, S.; Noonan, K. J. T. *Org. Lett.* **2013**, *15*, 5230−5233.
(32) (a) Amir, E.; Rozen, S. *Angew. Chem., Int. Ed.* **2005**, *44*, 7374−7378. (b) Shefer, N.; Harel, T.; Rozen, S. *J. Org. Chem.* **2009**, *71*, 6993−6998. (c) Potash, S.; Rosen, S. *J. Org. Chem.* **2011**, *76*, 7245−7248. (d) Oliva, M. M.; Casado, J.; Navarrete, J. T. L.; Patchkovskii, S.; Goodson, T., III; Harpham, M. R.; Seixas de Melo, J. S.; Amir, E.; Rozen, S. *J. Am. Chem. Soc.* **2010**, *132*, 6231−6242. (e) Potash, S.; Rozen, S. *Chem.—Eur. J.* **2013**, *19*, 5289−5296.
(33) Dosche, C.; Löhmannsröben, H.-G.; Bieser, A.; Dosa, P. I.; Han, S.; Iwamoto, M.; Schleifenbaum, A.; Vollhardt, K. P. C. *Phys. Chem. Chem. Phys.* **2002**, *4*, 2156−2161.
(34) (a) Farnum, D. G.; Atkinson, E. R.; Lothrop, W. C. *J. Org. Chem.* **1961**, *26*, 3204−3208. (b) Hochstrasser, R. M.; McAlpine, R. D. *J. Chem. Phys.* **1966**, *44*, 3325−3328. (c) Paradejordi, F.; Domingo, R.; Fernández-Alonso, J. I. *Int. J. Quantum Chem.* **1969**, *3*, 683−698. (d) Zanon, I. *J. Chem. Soc., Faraday Trans. 2* **1973**, *69*, 1164−1171. (e) Vogler, H.; Ege, G. *J. Am. Chem. Soc.* **1977**, *99*, 4599−4604. (f) Jørgensen, N. H.; Pedersen, P. B.; Thulstrup, E. W.; Michl, J. *Int. J. Quantum Chem.* **1978**, *S12*, 419−431. (g) Lin, H.-B.; Topp, M. *Chem. Phys. Lett.* **1979**, *64*, 452−456. (h) Ohta, N.; Fujita, M.; Baba, H.; Shizuka, H. *Chem. Phys.* **1980**, *47*, 389−394.
(35) Yamaguchi, H.; Ata, M.; McOmie, J. F. W.; Barton, J. W.; Baumann, H. *J. Chem. Soc., Faraday Trans. 2* **1983**, *79*, 599−609.
(36) Shizuka, H.; Ogiwara, T.; Cho, S.; Morita, T. *Chem. Phys. Lett.* **1976**, *42*, 311−314.
(37) Fleischhauer, J.; Höweler, U.; Spanget-Larsen, J.; Raabe, G.; Michl, J. *J. Phys. Chem. A* **2004**, *108*, 3225−3234.
(38) (a) Höweler, U.; Downing, J. W.; Fleischhauer, J.; Michl, J. *J. Chem. Soc., Perkin Trans. 2* **1998**, 1101−1117. (b) Fleischhauer, J.; Höweler, U.; Michl, J. *Spectrochim. Acta, Part A* **1999**, *55*, 585−606. (c) Fleischhauer, J.; Höweler, U.; Michl, J. *J. Phys. Chem. A* **2000**, *104*, 7762−7775.
(39) (a) Michl, J. *Tetrahedron* **1984**, *40*, 3845−3934. (b) Mack, J.; Stillman, M. J.; Kobayashi, N. *Coord. Chem. Rev.* **2007**, *251*, 429−453. (c) Kobayashi, N.; Muranaka, A.; Mack, J. *Circular Dichroism and Magnetic Circular Dichroism Spectroscopy for Organic Chemists*; Royal Society of Chemistry: Cambridge, UK, 2012.